Effects of fractional mass transfer and chemical reaction on MHD flow in a heterogeneous porous medium

Liu, Chunyan; Zheng, Liancun; Pan, Mingyang; Lin, Ping; Liu, Fawang

Published in:
Computers and Mathematics with Applications

DOI:
10.1016/j.camwa.2019.04.011

Publication date:
2019

Accepted Manuscript version of Liu, Chunyan et al. "Effects of fractional mass transfer and chemical reaction on MHD flow in a heterogeneous porous medium". Computers and Mathematics with Applications. 2019. https://doi.org/10.1016/j.camwa.2019.04.011

Effects of fractional mass transfer and chemical reaction on MHD flow in a heterogeneous porous medium

Chunyan Liu[a], Liancun Zheng[a,*], Mingyang Pan[b], Ping Lin[a,c], Fawang Liu[d]

[a]*School of Mathematics and Physics, University of Science and Technology Beijing, Beijing 100083, China*
[b]*School of Science and Engineering, The Chinese University of Hong Kong, Shenzhen, Shenzhen, Guangdong, 518172, P.R. China*
[c]*Division of Mathematics, University of Dundee, Dundee DD1 4HN, Scotland, United Kingdom*
[d]*School of Mathematical Sciences, Queensland University of Technology, GPO Box 2434, Brisbane, QLD. 4001, Australia*

Abstract

This paper presents a study on space fractional anomalous convective-diffusion and chemical reaction in the magneto-hydrodynamic fluid over an unsteady stretching sheet. The fractional diffusion model is derived from decoupled continuous time random walks in a heterogeneous porous medium. A novel transformation which features time finite difference is introduced to reduce the governing equations into ordinary differential ones in each time level. Numerical solutions are obtained by an implicit finite difference scheme. The stability and convergence of the method are analyzed. Results show that increasing fractional derivative parameter enhances concentration near the surface while an opposite phenomenon occurs far away from the surface. There is a reduction of mass transfer rate on the sheet with an increase in the fractional derivative parameter. Moreover, the numerical solutions are compared with exact solutions and good agreement has been observed.

Keywords: Heterogeneous porous medium, Anomalous diffusion, Unsteady stretching sheet, Finite difference method, Stability and convergence

1. Introduction

The investigation of boundary layer flow past a stretching sheet has received considerable attention in industrial applications, such as melt-spinning, hot rolling, manufacture of plastic and polymer sheets, etc. To be more specific, the fluid has been shown under a variety of circumstances, i.e., magnetic field [1], porous medium [2], mass diffusion [3] and others [4, 5] for the stretching problem. The above studies only take steady flow into consideration. However, the flow field should be unsteady, owing to sudden stretching of the flat sheet under external actions. Elbashbeshy et al. [6] considered the unsteady flow and heat transfer of the

*Corresponding author.Tel.:+86(10)6233 2002
Email address: liancunzheng@ustb.edu.cn, liancunzheng@163.com (Liancun Zheng)

laminar boundary layer over a horizontal stretching surface. Dandapat et al. [7] presented the influence of variable fluid thermophysical properties on the unsteady flow of a thin liquid film over a stretching sheet. Subsequently, a number of authors have studied the model of an unsteady stretching sheet in Refs. [8–11].

Recent works have shown that the fractional calculus theory has important applications in widespread fields of engineering and science [12, 13]. The traditional convection-diffusion equation combines the first time derivative and the second space derivative [14]. The fractional diffusion modifies the time or space derivatives with various fractional counterpart operators [15], which is distinct from the Gaussian diffusion. It is characterized by deviations from traditional linear time dependence in its mean square displacement e.g., $\langle (x - \langle x \rangle) \rangle^2 \sim t^\alpha$ with $\alpha \neq 1$, which relies on the non-Markovian features manifested by the systems [16]. Space fractional derivatives for $1 < \alpha < 2$, correspond to long power-law particle jumps, while time fractional derivatives for $0 < \alpha < 1$, correspond to long power-law waiting times between particle jumps [17]. Based on the applications of fractional derivatives in time or space, various studies are carried out to simulate the thermal transport and mass diffusion of particles [18–20].

It is known that diffusion in porous media is of current attention to the scientific and technical applications. This interest arises because of the influence of oil recovery, subsurface contamination and moisture dispersion in building materials [21–23]. The classical experimental results have shown non-Fickian dispersion processes in heterogeneous porous media [24]. Complex geometries in porous media may be considered as random fractal [25]. Continuous time random walks (CTRWs) become helpful tools in the assessment of dispersive processes in heterogeneous porous media [26], which are introduced in [27]. The CTRWs have also been applied in the analysis of diffusion behaviors in a porous medium by other scholars [28, 29]. Motivated by the above discussions, the objective of this paper is to study the anomalous diffusion in magneto-hydrodynamic (MHD) flow through a heterogeneous porous medium over an unsteady stretching sheet. Applications of the present study are also useful in chemical engineering systems. The fractional diffusion model is derived from the stochastic theory of decoupled CTRWs.

The structure of the paper is organized as follows: in Section 2, physical backgrounds and mathematical modeling are proposed. The derivation of transformation featuring time finite difference for the governing equations is presented in Section 3. In Section 4, the set of equations are solved by using bvp4c and implicit finite difference method (IFDM) and stability and convergence of IFDM are strictly proved. The analyses of results and discussions are given in Section 5, followed by conclusions in Section 6. Finally, the derivation of the space fractional diffusion model is depicted in Appendix.

Nomenclature

a	stretching rate, $[m\ s^{-1}]$
B_0	magnetic flux density, $[T]$
C	concentration, $[kg\ m^{-3}]$
C_f	skin friction coefficient, $[-]$
C_w	concentration at stretching surface, $[kg\ m^{-3}]$
C_∞	ambient concentration, $[kg\ m^{-3}]$
D	mass diffusivity, $[m^2\ s^{-1}]$
F	similar stream function, $[-]$
H_m	convective mass coefficient, $[m\ s^{-1}]$
K	permeability of the porous medium, $[m^2]$
M	Hartmann number, $[-]$
q_m	wall mass flux, $[kg\ m^{-2}s^{-1}]$
R	dimensionless chemical reaction parameter, $[-]$
Re_x	local Reynolds number, $[-]$
Sc	Schmidt number, $[-]$
Sh_x	local Sherwood number, $[-]$
t	dimensionless time parameter, $[-]$
u,v	velocity in x,y-axis direction, $[m\ s^{-1}]$
u_w	stretching sheet velocity, $[m\ s^{-1}]$
$\vec{\mathbf{u}}$	velocity vector, $[m\ s^{-1}]$
x,y	x,y-axis, $[m]$
Greek symbols	
β	fractional derivative parameter, $[-]$
η	similarity variable, $[-]$
ξ	similarity variable after coordinate transformation, $[-]$
ϕ	dimensionless variable of C, $[-]$
ψ	stream function, $[m^2\ s^{-1}]$
μ	dynamic viscosity of fluid, $[Nsm^{-2}]$
ν	kinematic viscosity, $[m^2\ s^{-1}]$
ρ	density of fluid, $[kg\ m^{-3}K]$
σ	electrical conductivity of fluid, $[S\ m^{-1}]$
τ	dimensionless time step, $[-]$
τ_1	dimensional balance ratio, $[m^{\beta-2}]$
τ_w	wall shear stress, $[N\ m^{-2}]$
Ω	porosity parameter, $[-]$
ϖ	scaled convective mass transfer parameter, $[-]$
Subscripts	
w	condition at the surface, $[-]$
∞	ambient condition, $[-]$
f	fluid, $[-]$

Superscript	
$'$	differentiation with respect to η or ξ, $[-]$

2. Geometry and mathematical modeling

We consider the two-dimensional unsteady flow of MHD fluid due to a stretching sheet with the linear velocity $u_w = ax$, $(a > 0)$. The mass transfer process is governed by the fractional convection-diffusion equation in a heterogeneous porous medium. The concentration of stretching surface is given by convection form, which is characterized by a high concentration C_w and a convective mass transfer coefficient H_m. Furthermore, the first-order chemical reaction takes place in the flow. Since the magnetic Reynolds number is assumed to be small enough for most conducting fluids used in industrial applications, the induced magnetic field can be negligible. The physical model and coordinate system are shown in Fig. 1. The governing equations for the continuity, momentum and concentration in laminar boundary layer are presented, respectively, as follows:

$$\nabla \cdot \vec{\mathbf{u}} = 0, \tag{1}$$

$$\rho \frac{\partial \vec{\mathbf{u}}}{\partial t} + \rho(\vec{\mathbf{u}} \cdot \nabla)\vec{\mathbf{u}} = \mu \nabla^2 \vec{\mathbf{u}} - (\mu/K)\vec{\mathbf{u}} - \sigma B_0^2 \vec{\mathbf{u}}, \tag{2}$$

$$\frac{\partial C}{\partial t} + \vec{\mathbf{u}} \cdot \nabla C = \tau_1^{\beta-2} D \cdot D_y^{\beta} C - R(C - C_\infty). \tag{3}$$

We write $\vec{\mathbf{u}} = (u, v)$. Here u and v are velocity components in the directions of x and y, ρ refers to the fluid density and t is the time variable. μ means the viscosity, σ is the electrical conductivity of the fluid and B_0 is the magnetic flux density. D is the mass diffusivity, K is the permeability of porous medium, C_∞ is the ambient concentration and R is the chemical reaction coefficient. The additional coefficient τ_1 is introduced to balance the dimension and we set $\tau_1 = 1$ in the following discussion. The Caputo fractional derivative with $1 < \beta < 2$ is defined as [30]

$$D_y^{\beta} C = \frac{\partial^{\beta} C}{\partial y^{\beta}} = \frac{1}{\Gamma(2-\beta)} \int_0^y (y-\zeta)^{1-\beta} \frac{\partial^2 C}{\partial y^2} d\zeta. \tag{4}$$

The initial and boundary conditions are

$$t \le 0 : u(x,y,t) = v(x,y,t) = 0, C(x,y,t) = C_\infty \quad \text{as} \quad y > 0, \tag{5}$$

$$t > 0 : \begin{cases} u_w(x,t) = ax, v(x,t) = 0, -D\frac{\partial C}{\partial y} = H_m(C_w - C) \quad \text{as} \quad y = 0 \\ u(x,t) = 0, C(x,t) = C_\infty \quad \text{as} \quad y \to \infty \end{cases}, \tag{6}$$

where a represents a positive constant.

The following dimensionless variables are introduced

$$\begin{gathered} x^* = \frac{x}{\sqrt{\nu/a}}, y^* = \frac{y}{\sqrt{\nu/a}}, t^* = \frac{t}{1/a}, u^* = \frac{u}{\sqrt{a\nu}}, v^* = \frac{v}{\sqrt{a\nu}}, \\ \hat{\phi}^* = \frac{C - C_\infty}{C_w - C_\infty}, R^* = \frac{R}{a}, M = \frac{\sigma B_0^2}{a\rho}, \Omega = \frac{\nu}{aK}. \end{gathered} \tag{7}$$

Substituting (7) into (1)-(6), then we obtain the following nonlinear partial differential equations (here we omit the superscript $*$ for simplicity)

$$\frac{\partial u}{\partial x}+\frac{\partial v}{\partial y}=0, \tag{8}$$

$$\frac{\partial u}{\partial t}+u\frac{\partial u}{\partial x}+v\frac{\partial u}{\partial y}=\frac{\partial^2 u}{\partial y^2}-(M+\Omega)u, \tag{9}$$

$$\frac{\partial \hat{\phi}}{\partial t}+u\frac{\partial \hat{\phi}}{\partial x}+v\frac{\partial \hat{\phi}}{\partial y}=\frac{1}{Sc}\frac{\partial^\beta \hat{\phi}}{\partial y^\beta}-R\hat{\phi}. \tag{10}$$

The nondimensional initial and boundary conditions are

$$t\leq 0: u=v=0, \hat{\phi}=0 \quad \text{as} \quad y>0, \tag{11}$$

$$t>0: \begin{cases} u=x, v=0, \hat{\phi}=1+\tilde{\varpi}\frac{\partial \hat{\phi}}{\partial y} & \text{as} \quad y=0 \\ u=0, \hat{\phi}=0 & \text{as} \quad y\to\infty \end{cases}, \tag{12}$$

where $Sc=\nu/D$ is the Schmidt number, $\tilde{\varpi}=D/H_m$ is the convective mass transfer parameter, Ω is the porosity parameter, M is the Hartmann number, and R is the chemical reaction parameter.

3. A novel transformation featuring time finite difference

For sake of calculation simplicity, we replace the partial derivatives $\partial u/\partial t$, and $\partial\hat{\phi}/\partial t$ of unknown functions u, and $\hat{\phi}$ by the difference quotients $(u_n-u_{n-1})/\tau$, and $(\hat{\phi}_n-\hat{\phi}_{n-1})/\tau$, respectively, where τ is the time step [31]. Eqs. (8)-(10) can be written as

$$\frac{\partial u_n}{\partial x}+\frac{\partial v_n}{\partial y}=0, \tag{13}$$

$$\frac{u_n-u_{n-1}}{\tau}+u_n\frac{\partial u_n}{\partial x}+v_n\frac{\partial u_n}{\partial y}=\frac{\partial^2 u_n}{\partial y^2}-(M+\Omega)u_n, \tag{14}$$

$$\frac{\hat{\phi}_n-\hat{\phi}_{n-1}}{\tau}+u_n\frac{\partial \hat{\phi}_n}{\partial x}+v_n\frac{\partial \hat{\phi}_n}{\partial y}=\frac{1}{Sc}\frac{\partial^\beta \hat{\phi}_n}{\partial y^\beta}-R\hat{\phi}_n. \tag{15}$$

Here u_n, $\hat{\phi}_n$ represent the unknown solutions of nth time level and u_{n-1}, $\hat{\phi}_{n-1}$ represent the known quantity of n-1th time level.

To obtain the solutions, we define the stream function ψ satisfying $u=\partial\psi/\partial y$ and $v=-\partial\psi/\partial x$. We introduce the following dimensionless functions F, $\hat{\phi}$ and the similarity variable η as [32]

$$\eta=y, \psi=xF(\eta), \hat{\phi}=\hat{\phi}(\eta). \tag{16}$$

Using (16), Eqs. (13)-(15) reduce to the following nondimensional forms

$$(\tau M + \tau\Omega + 1)F_n' + \tau F_n'^2 - \tau F_n F_n'' - \tau F_n''' = F_{n-1}', \tag{17}$$

$$(1 + \tau R)\hat{\phi}_n - \tau F\hat{\phi}_n' - \frac{\tau}{Sc} D_\eta^\beta \hat{\phi}_n = \hat{\phi}_{n-1}, \tag{18}$$

subject to the initial and boundary conditions

$$t \leq 0 : F' = F = 0, \hat{\phi} = 0 \quad \text{as} \quad \eta > 0, \tag{19}$$

$$t > 0 : \begin{cases} F_n' = 1, F_n = 0, \hat{\phi}_n = 1 + \varpi\hat{\phi}_n' & \text{as} \quad \eta = 0 \\ F_n' = 0, \hat{\phi}_n = 0 & \text{as} \quad \eta \to \infty \end{cases}. \tag{20}$$

The primes denote derivative with respect to η. The ambient condition of (20) is usually replaced in numerical method by the suitable finite value

$$F_n' = 0, \hat{\phi}_n = 0, \quad \text{as} \quad \eta \to \eta_0. \tag{21}$$

We exploit the coordinate transform $\eta = \eta_0\xi$, then (17) and (18) become

$$(\tau M + \tau\Omega + 1)f_n' + \frac{\tau}{\eta_0} f_n'^2 - \frac{\tau}{\eta_0} f_n f_n'' - \frac{\tau}{\eta_0^2} f_n''' = f_{n-1}', \tag{22}$$

$$(1 + \tau R)\phi_n - \frac{\tau}{\eta_0} f_n \phi_n' - \frac{\tau}{\eta_0^\beta Sc} D_\xi^\beta \phi_n = \phi_{n-1}. \tag{23}$$

The initial and boundary conditions are given by

$$t \leq 0 : f' = f = 0, \phi = 0 \quad \text{as} \quad \xi > 0, \tag{24}$$

$$t > 0 : \begin{cases} f_n' = \eta_0, f_n = 0, \phi_n = 1 + \varpi\phi_n' & \text{as} \quad \xi = 0 \\ f_n' = 0, \phi_n = 0 & \text{as} \quad \xi = 1 \end{cases}, \tag{25}$$

where $\varpi = \tilde{\varpi}/\eta_0$ is the scaled convective mass transfer parameter and the primes denote the differentiation with respect to the similarity variable ξ. The quantities of practical interest in this paper are the skin friction coefficient C_f and the local Sherwood number Sh_x, which are defined as

$$C_f = \frac{\tau_w}{\rho u_w^2}, Sh_x = \frac{x q_m}{D(C_w - C_\infty)}. \tag{26}$$

τ_w is the wall shear stress and q_m is the mass flux at the stretching surface, which are given by

$$\tau_w = \mu \left.\frac{\partial u}{\partial y}\right|_{y=0}, q_m = -D \left.\frac{\partial C}{\partial y}\right|_{y=0}. \tag{27}$$

The skin friction coefficient C_f and the local Sherwood number Sh_x are obtained as

$$C_f Re_x^{1/2} = F''(0), Sh_x/Re_x^{1/2} = -\phi'(0), \tag{28}$$

where $Re_x = x u_w/\nu$ is the local Reynolds number.

4. Numerical technique

4.1. The novel transformation

The governing equations (13)-(15) are transformed into ordinary differential equations (ODEs) with regard to each time level (17)-(18) using novel transformation. Unlike the traditional similarity transformation, this novel transformation featuring time difference provides an effective method for solving space fractional partial differential equations of unsteady boundary layer model.

4.2. The discretization of the convection anomalous diffusion problem

Consider $\xi_n = \tau n$ for $n = 0, 1, \cdots, N_\tau$ and a truncation error $o(\tau)$ of the difference in time before similarity transformation. Set $h = 1/N$, $\xi_j = jh$, for $j = 0, 1, ..., N$. Then, to discretize $-D_\xi^\beta \phi_n$ and ϕ_n' in (23), we use the classical L2 approximation of $-D_\xi^\beta \phi_n(\xi_j) = -\frac{1}{h^\beta \Gamma(3-\beta)} \sum_{k=0}^{j-1} d_{j-k}(\phi_{k+2}^n - 2\phi_{k+1}^n + \phi_k^n) + O(h)$ [33] and forward difference approximation of $\phi_n'(\xi_j) = (\phi_{j+1}^n - \phi_j^n)/h + O(h)$, respectively, where ϕ_k^n denotes the computed approximation to $\phi_n(\xi_k)$. We set $d_r = r_+^{2-\beta} - (r-1)_+^{2-\beta}$ for all integers r, with

$$s_+ = \begin{cases} s \ if \ s \geq 0, \\ 0 \ if \ s < 0. \end{cases} \tag{29}$$

The full discretization of (23) is

$$-\frac{\tau}{Sc\eta_0^\beta h^\beta \Gamma(3-\beta)} \sum_{k=0}^{j-1} d_{j-k}(\phi_{k+2}^n - 2\phi_{k+1}^n + \phi_k^n) - \frac{\tau f_j^n}{\eta_0} \frac{\phi_{j+1}^n - \phi_j^n}{h} + (1 + \tau R)\, \phi_j^n = \phi_j^{n-1} \tag{30}$$

for $j = 1, 2, ...N-1$ and $n = 1, 2, ..., N_\tau$.

Remark 1. The implicit finite difference scheme of (30) has a local truncation error of e_r=$O(h + \tau)$.

Eqs. (30), (24) and (25) can be written in matrix form

$$A\vec{\phi}^n = \vec{\phi}^{n-1}. \tag{31}$$

$\phi_n'(0)$ of the boundary condition (25) is discretized by forward difference approximation of $\phi_n'(0) = (\phi_1^n - \phi_0^n)/h + O(h)$.

The unknowns $\vec{\phi}^n := (\phi_0^n, \phi_1^n, \cdots, \phi_N^n)^T$ are the solutions in nth time level of the linear system (31). $\vec{\phi}^{n-1}$:= $(1, \phi_1^{n-1}, \phi_2^{n-1}, \cdots, \phi_{N-1}^{n-1}, 0)^T$ are the variables of n-1th time level, which are treated as constants. $A = (a_{jk})_{j,k=0}^N$ denotes a $(N+1) \times (N+1)$ matrix corresponding to the discretization (24), (25) and (30). The 0th row of A is $(1 + \varpi h^{-1}, -\varpi h^{-1}, 0, \cdots, 0)$

and its Nth row is $(0, 0, \cdots, 1)$. For $j = 1, 2, \ldots, N-1$, $k = 2, 3, \cdots, N$, the entries of the jth row of A satisfy

$$\begin{aligned} a_{j0} =& \frac{-d_j}{\tau^{-1} Sc \eta_0^{\beta} h^{\beta} \Gamma(3-\beta)}, \\ a_{j1} =& \frac{-d_{j-1} + 2d_j}{\tau^{-1} Sc \eta_0^{\beta} h^{\beta} \Gamma(3-\beta)} + \delta_{j1} \left[\frac{\tau f_1^n}{h\eta_0} + (1 + \tau R) \right], \\ a_{jk} =& \frac{-d_{j-k} + 2d_{j-k+1} - d_{j-k+2}}{\tau^{-1} Sc \eta_0^{\beta} h^{\beta} \Gamma(3-\beta)} + \delta_{jk} \left[\frac{\tau f_j^n}{h\eta_0} + (1 + \tau R) \right] - \delta_{j,k-1} \frac{\tau f_j^n}{h\eta_0}, \end{aligned} \tag{32}$$

where R satisfies $R > 0$ for physical characteristics of the model. We set

$$\delta_{jk} = \begin{cases} 1 & if\ j = k \\ 0 & otherwise \end{cases}. \tag{33}$$

The non-zero entries of A satisfy various inequalities [34–36],

$$\begin{aligned} & a_{00} > 0, a_{01} < 0, a_{N,N-1} = 0, a_{NN} = 1, a_{jj} > 0, \text{ for all } j, \\ & a_{j0} < 0 \text{ for } j = 1, 2, \ldots, N-1, a_{j1} > 0 \text{ for } j = 2, 3, \ldots, N-1, \\ & a_{jk} < 0 \text{ for } j = 1, 2, \ldots, N-1 \text{ and } k = 2, 3, \ldots, j-2, j-1, j+1. \end{aligned} \tag{34}$$

4.3. Monotonicity of the discretization matrix A

To ensure that A is invertible and admit the important inequality $A^{-1} \geq 0$. The positive off-diagonal entries in column 1 of matrix A become limitations for further analysis [34, 35]. So we multiply A by elementary row transformation matrices $E^{(k)} := (e_{ij}^{(k)})_{i,j=0}^{N}$, where

$$e_{ij}^{(k)} = \epsilon_{ij} - \frac{a_{k0}}{a_{00}} \epsilon_{ik} \epsilon_{j0}. \tag{35}$$

Let

$$A' = E^{(N-1)} E^{(N-2)} \cdots E^{(1)} A, \tag{36}$$

and denote $A' = (a'_{jk})_{j,k=0}^{N}$. Row 0 of A' is $(a_{00}, a_{01}, 0, \cdots, 0)$. By this technique $a'_{j0} = 0$ for $j = 1, 2, \ldots, N-1$. For $k \geq 2$ and all j, we clearly obtain $a'_{jk} = a_{jk}$. $a'_{11} > 0$ and $a'_{j1} < 0$ for $j = 2, 3, \ldots, N-1$ can be proved in [34].

Lemma 4.1. *A' is an M-matrix. Furthermore, A is invertible and $A^{-1} \geq 0$, thus the matrix A is monotone.*

Proof. The matrix A' has positive diagonal entries and nonpositive off-diagonal entries. It is easy to validate that $\sum_{k=0}^{N} a'_{0k} = \sum_{k=0}^{N} a'_{Nk} = 1$. With $\sum_{k=0}^{N} a_{jk} = 1 + \tau R$, $(R > 0)$,

one has

$$\begin{aligned}\sum_{k=0}^{N} a'_{jk} &= 0 + (a_{j1} + \frac{\varpi h^{-1}}{1+\varpi h^{-1}} a_{j0}) + \sum_{k=2}^{N} a_{jk} \\ &= (\frac{\varpi h^{-1}}{1+\varpi h^{-1}} - 1) a_{j0} + \sum_{k=0}^{N} a_{jk} \\ &= (\frac{\varpi h^{-1}}{1+\varpi h^{-1}} - 1) a_{j0} + (1+\tau R) \\ &> 0\end{aligned} \tag{37}$$

for $j = 1, 2, \ldots, N-1$. Thus there exists a vector $\vec{w}:=(1, 1, \cdots, 1)^T$, subject to $A'\vec{w} > \vec{0}$. Consequently, A' is an M-matrix and $(A')^{-1} \geq 0$. By (36), we have

$$A^{-1} = (A')^{-1} E^{(N-1)} E^{(N-2)} \cdots E^{(1)}, \tag{38}$$

which implies that A^{-1} exists and $A^{-1} \geq 0$, thus matrix A is monotone. □

4.4. Stability and convergence

Lemma 4.2. *A is a monotone matrix of order $N+1$ and there exists a vector $\vec{w}:=(1, 1, \cdots, 1)^T$ with $\|\vec{w}\|_\infty = 1$ such that $(A\vec{w})_0 = 1$, $(A\vec{w})_N = 1$ and $(A\vec{w})_i = 1+\tau R$ for $i = 1, 2, \ldots, N-1$. Then $\|A^{-1}\|_\infty \leq 1$ [37].*

Proof. Let $A^{-1} = (\tilde{a}_{ij})_{i,j=0}^{N}$. Since $I = A^{-1}A$ we have

$$\begin{aligned}1 = &\|\vec{w}\|_\infty = \vec{w}_i = (A^{-1}A\vec{w})_i = \sum_{j=0}^{N} \tilde{a}_{ij} (A\vec{w})_j \\ &\geq \sum_{j=0}^{N} \tilde{a}_{ij} = (A^{-1}\vec{w})_i\end{aligned} \tag{39}$$

for $i = 0, 1, \cdots, N$, and note that

$$\|A^{-1}\|_\infty = \|A^{-1}\vec{w}\|_\infty, \tag{40}$$

which yields

$$\|A^{-1}\|_\infty = \max_i (A^{-1}\vec{w})_i \leq 1. \tag{41}$$

□

Theorem 4.1. *(stability of the IFDM) The implicit finite difference method of (30) is unconditionally stable.*

Proof. We rewrite (30) as

$$\vec{\phi}^n = A^{-1}\vec{\phi}^{n-1}. \tag{42}$$

We suppose that $\tilde{\phi}^n$ is an approximate solution of (42). The error $\epsilon^n = \tilde{\phi}^n - \vec{\phi}^n$ satisfies

$$\epsilon^n = A^{-1}\varepsilon^{n-1}. \tag{43}$$

From lemma 4.2,

$$\|\epsilon^n\|_\infty = \|A^{-1}\varepsilon^{n-1}\|_\infty \leq \|A^{-1}\|_\infty \|\varepsilon^{n-1}\|_\infty \leq \|\varepsilon^{n-1}\|_\infty. \tag{44}$$

Applied (44) repeatedly n times, we obtain

$$\|\varepsilon^n\|_\infty \leq \|\varepsilon^0\|_\infty. \tag{45}$$

Therefore the implicit numerical method defined by (30) is unconditionally stable. □

Theorem 4.2. *(convergence of the IFDM) The implicit finite difference method of (30) is convergent, and the order of convergence is $O(\tau + h)$.*

Proof. To discuss the convergence of the numerical method, let us suppose that $e_j^n = \vec{\phi}(\eta_j, t_n) - \vec{\phi}_j^n$ and $e^n := (e_1^n, e_2^n, \cdots, e_{j-1}^n)^T$. Using the initial boundary conditions $e_j^0 = 0$, $e_0^n = \varpi/(\varpi + h)e_1^n$, $e_N^n = 0$, we obtain the following error equation

$$e^n = A^{-1}e^{n-1} + M, \tag{46}$$

and $e^0 = 0$, where $M = \tau(O(\tau + h))(1, 1, \cdots, 1)^T$.
Hence we get the following error equation

$$e^n = ((A^{-1})^n + (A^{-1})^{n-1} + \cdots + (A^{-1})^2 + (A^{-1})^1 + I)M. \tag{47}$$

Then

$$\begin{aligned} &\|e^n\|_\infty \\ \leq &(\|(A^{-1})^n\|_\infty + \|(A^{-1})^{n-1}\|_\infty + \cdots + \|(A^{-1})^1\|_\infty + \|I\|_\infty)\|M\|_\infty. \end{aligned} \tag{48}$$

Using lemma 4.2,

$$\|e^n\|_\infty \leq (n+1)\tau|O(\tau + h)|. \tag{49}$$

Consequently, the implicit numerical method defined by (30) is convergent. □

4.5. Accuracy and effectiveness of the algorithm

In the computation we choose parameters $\tau = 0.01$ and $N = 300$. It is assumed that the velocity F and concentration ϕ have no significant changes after less than 10^{-4} at all grid points in adjacent time steps. The value of η_0 is taken as 5 to satisfy the boundary condition (25). It is noted that velocity profiles with similarity variable η are shown in Figs. 2-4, while concentration profiles after coordinate transformation with similarity variable ξ in order to fit in with the IFDM are presented in Figs. 5-6. When the steady state is reached, the velocity equation (17) with the boundary conditions $F'(0) = 1, F(0) = 0$ and $F'(\infty) = 0$ in (20) suggests a exact solution [38]:

$$F(\eta) = \frac{1}{\sqrt{1+M+\Omega}}(1 - e^{-\eta\sqrt{1+M+\Omega}}). \tag{50}$$

In this paper, we present the bvp4c to solve it numerically for different values of Hartmann number M and porosity parameter Ω. The comparisons of numerical solutions of steady state ($t = 6$) and exact solutions for velocity profiles are presented in Fig. 2. It is important to note that the numerical results agree well with the exact solutions. Furthermore, the results effectively show that the method of transformation featuring time finite difference (13)-(15) is correct. It is indicated in Fig. 5 that the comparisons of solid line by IFDM and dashed line by bvp4c for concentration profiles in $\beta = 2$ are made. Excellent agreement is obtained as expected.

5. Results and Discussions

In this paper, the fractional convection-diffusion in unsteady MHD fluid flow through a heterogeneous porous medium with first-order chemical reaction is investigated. The effects of involved physical parameters on velocity and concentration fields are analyzed in detail, such as Hartmann number M, porosity parameter Ω, time parameter t, fractional derivative parameter β, scaled convective mass transfer parameter ϖ, and Schmidt number Sc. Then the variations of skin friction coefficient C_f and local Sherwood number Sh_x are examined.

Fig. 3 illustrates the impacts of Hartmann number M on the conducting fluid flow with the conditions $\Omega = 0.1, Sc = 5, R = 0.2, \varpi = 1.1, \beta = 1.9$ and $t = 0.5$. By assuming Hartmann number M=0, the values of velocity are higher than that of the case, where a vertical magnetic field is applied to the conducting fluid. The Lorentz force is generated by the vertical magnetic field in conducting fluid, which tends to slow fluid flow. Therefore the velocity of the MHD fluid is reduced with the increase of Hartmann number. One can see that the velocity boundary layer thickness gets depressed slightly with the enhancement in the Hartmann parameter physically. The effects of a continuous change of time parameter on velocity distributions at different spatial positions are shown in Fig. 4. It is clear that the velocity profiles increase until reaching steady with the enlargement of time parameter. Moreover, the velocity closer to the wall becomes larger at all the fixed unsteady time and it takes to reach the maximum velocity in a shorter time. It is noted that the fluid velocity decreases with the increment of η because of the effect of stretching flow.

Fig. 5 reveals the effects of fractional derivative parameter β on concentration profiles. The concentration distribution decreases with the increasing fractional derivative parameter near the surface, but the opposite trend occurs far away from the surface. This is because the fractional anomalous diffusion takes into account nonlocality and the fractional model is able to more accurately simulate heavy-tailed motions than the standard model. It can be further obtained that the concentration gradient increases, while the thickness of concentration boundary layer becomes thinner with the augments of β. Fig. 6 displays the effects of the continuous change of time parameter on concentration distribution at different spatial positions. From this figure, one can see that the concentration profiles of the MHD fluid are decreased with the increase in the similarity variable ξ. The fastest change in the concentration occurs in the case of $\xi = 0.05$. In addition, the concentration change slows down with the increase of distance from the wall. It is concluded that the increase in time parameter causes an increase in concentration profiles.

Fig. 7 depicts that the effect of Schmidt number Sc and the scaled convective mass transfer parameter ϖ on the local Sherwood number Sh_x. It is observed that the local Sherwood number decreases with increasing values of the scaled convective mass transfer parameter. Moreover, larger Schmidt number corresponds to higher local Sherwood number. That is to say, increasing Schmidt number leads to the increase of mass transfer on the sheet. Table 1 shows the skin friction coefficient distributions for different Hartmann number M and porosity parameter Ω, when the other parameters are fixed ($Sc = 5, R = 0.2, \beta = 1.9$, and $\varpi = 1.1$). With the augments of M and Ω, skin friction coefficient increases obviously. So Lorenz force hinders MHD fluid flow on the sheet and with the increase of porosity parameter, the friction on the wall is enhanced. The local Sherwood number distributions for different chemical reaction parameter R and fractional derivative parameter β are presented in Table 2 with $M = 0.1, \Omega = 0.1, R = 0.2$, and $\varpi = 1.1$. The local Sherwood number increases as the chemical reaction parameter rises, but decreases with the augments of fractional derivative parameter. These results demonstrate that the fractional derivative parameter reduces the mass transfer clearly, i.e., anomalous diffusion reduces the mass transfer rate at the surface, while the chemical reaction improves the mass transfer rate at the surface.

6. Conclusions

The unsteady flow and mass transfer of an incompressible MHD fluid over a moving plate are studied in the present paper. Anomalous diffusion in a heterogeneous porous medium is also considered. Under the condition of chemical reaction, the momentum equation together with the concentration equation is converted into ordinary differential forms by using the novel transformation featuring time finite difference. Numerical solutions are obtained by using bvp4c and IFDM in symbolic computation software. Stability and convergence of the IFDM are established. The effects of physical parameters on the flow, anomalous diffusion characteristics in the boundary layer, the skin friction coefficient, and the local Sherwood number are discussed in detail. From the computations and discussions above, we can draw the following conclusions:

(I) The fractional derivative parameter exerts significant influences on the concentration field. The thickness of concentration boundary layer becomes thinner with the increase of the fractional derivative parameter. Increasing fractional derivative parameter enhances concentration near the surface, but the opposite behavior occurs far away from the surface.

(II) Due to the application of the novel transformation featuring time finite difference, the system of space fractional partial differential equations is reduced to the numerical problem of ODEs for each time level.

(III) The velocity closer to the stretching sheet becomes larger on the unsteady-state time and it reaches the maximum velocity in a shorter time.

(IV) The local Sherwood number increases as the chemical reaction parameter rises, but decreases by the increasing values of fractional derivative parameter.

Acknowledgments

The work of the authors is supported by the National Natural Science Foundations of China (nos. 11772046, 81870345, 11771040, 11861131004).

7. Appendix-Derivation of the space fractional diffusion equation

Now we outline the argument for the stochastic theory of CTRWs. Let $\Psi(\mathbf{r},t)$ be the probability distribution of making a step of length $\mathbf{r}$ in a time between t and $t+dt$. The total transition probability in $(t,t+dt)$ is [39–42]

$$\Psi(t)=\sum_{\mathbf{r}}\Psi(\mathbf{r},t)=\Psi(\mathbf{k}=0,t). \tag{51}$$

$\Phi(t)$ is the survival probability that the interval $(0,t)$ is empty

$$\Phi(t)=1-\int_0^t\Psi(\tau)d\tau. \tag{52}$$

The conditional probability density $\tilde{\eta}(\mathbf{r},t)$ of being at position $\mathbf{r}$ in the interval between t and $t+dt$ is given by

$$\tilde{\eta}(\mathbf{r},t)=\sum_{\mathbf{r}'}\int_0^t\tilde{\eta}(\mathbf{r}',t)\Psi(\mathbf{r}-\mathbf{r}',t-\tau)d\tau+\delta_R(t)\delta_{\mathbf{r},0} \tag{53}$$

in which the initial condition of the random walk at position $\mathbf{r}=0$ at time $t=0$ is incorporated. From using $\tilde{\eta}(\mathbf{r},t)$ it follows that we can write the probability $C(\mathbf{r},t)$ of the particle at place $\mathbf{r}$ at time t

$$C(\mathbf{r},t)=\int_0^t\tilde{\eta}(\mathbf{r},t-\tau')\Phi(\tau')d\tau'. \tag{54}$$

The probability $C(\mathbf{r},t)$ applys (53) and (54) along with a change in the order of the integrations to get

$$C(\mathbf{r},t)=\sum_{\mathbf{r}'}\int_0^t C(\mathbf{r}',\tau)\Psi(\mathbf{r}-\mathbf{r}',t-\tau)d\tau+\Phi(t)\delta_{\mathbf{r},0}. \tag{55}$$

In Fourier-Laplace space (55) is derived

$$C(\mathbf{k},\omega)=C(\mathbf{k},\omega)\Psi(\mathbf{k},\omega)+\Phi(\omega). \tag{56}$$

The result can be obtained

$$C(\mathbf{k},\omega)=\frac{1-\Psi(\omega)}{\omega}\frac{1}{1-\Psi(\mathbf{k},\omega)}. \tag{57}$$

Now, we assume that space and time behaviors of CTRWs form are independent, i.e., $\Psi(\mathbf{r},t)=\phi_R(t)\lambda_R(\mathbf{r})$. The decoupled CTRWs process is characterized by the characteristic waiting time and the jump length variance [43]

$$\tau_R=\int_0^\infty dt\,t\int_{-\infty}^\infty \Psi(\mathbf{r},t)d\mathbf{r}\quad\text{and}\quad\sigma_R^2=\int_0^\infty dt\int_{-\infty}^\infty \mathbf{r}^2\Psi(\mathbf{r},t)d\mathbf{r}. \tag{58}$$

We choose $\sigma_R^2=\infty$ as Lévy jump length distribution and $\tau_R<\infty$ as Poissonian waiting time, i.e.,

$$\lambda_R(\mathbf{k})=e^{-\sigma_R^\beta|\mathbf{k}|^\beta}\sim 1-\sigma_R^\beta|\mathbf{k}|^\beta\quad\text{and}\quad\lambda_R(\mathbf{r})\sim\sigma_R^{-\beta}|\mathbf{r}|^{-1-\beta},\quad 1<\beta<2,|\mathbf{r}|\gg\sigma_R. \tag{59}$$

Substituting the asymptotic expansion form (59) into (57), we obtains

$$C(\mathbf{k},\omega)=\frac{1}{\omega+D|\mathbf{k}|^\beta}, \tag{60}$$

where $D=\sigma_R^\beta/\tau_R$ is the diffusion coefficient and the dimension of D is $cm^\beta s^{-1}$. Taking Fourier-Laplace inversion, we obtain the space fractional diffusion equation

$$\frac{\partial C}{\partial t}=D\cdot\nabla_{\mathbf{r}}^\beta C(\mathbf{r},t). \tag{61}$$

For Lévy flights in an external velocity field v, the fractional advection-diffusion equation (ADE) are given in a similar way [44, 45]

$$C(\mathbf{k},\omega)=\frac{1}{\omega+iv\mathbf{k}+D|\mathbf{k}|^\beta}. \tag{62}$$

In (x,t) space,

$$\frac{\partial C}{\partial t}+v\frac{\partial C}{\partial x}=D\cdot\nabla_x^\beta C(x,t). \tag{63}$$

Walks fit a heavy-tailed probability distribution ($\beta < 2$) between computations and validation experiments [46, 47]. If $\beta = 2$, (63) becomes the classical ADE. Besides, the derived equation is often represented by fractional derivatives in the Riemann-Liouville sense. However, the Caputo derivative often appears in applications. There is a general relation between the Caputo and Riemann-Liouville forms. To see this, some basic definitions and useful relations which are of relevance on fractional calculus are given as follows. Let $0 < x \leq 1$ and $m - 1 < n < m$, $(n \in \mathbb{R})$. The Riemann-Liouville fractional derivative ${}^{RL}\mathcal{D}^n$ is defined as [48]

$$ {}^{RL}\mathcal{D}_x^n g(x) = \frac{1}{\Gamma(m-n)} \frac{d^m}{dx^m} \int_0^x (x-t)^{m-n-1} g(t) dt \ , \tag{64} $$

where $\Gamma(x) = \int_0^\infty t^{x-1} e^{-t} dt$ is the Gamma function. An alternative definition is the Caputo fractional derivative $\mathcal{D}^n$, which is defined in terms of ${}^{RL}\mathcal{D}^n$ by [49]

$$ \mathcal{D}_x^n g(x) = {}^{RL}\mathcal{D}_x^n [g - T_{m-1}[g; 0]] = \frac{1}{\Gamma(m-n)} \int_0^x (x-t)^{m-n-1} g^{(m)}(t) dt \ , \tag{65} $$

where $T_{m-1}[g; 0]$ is the Taylor polynomial of degree $m - 1$ for $g(x)$ centered at $x = 0$. Therefore, in the manuscript, we study the fractional convection-diffusion equation with the Caputo fractional derivative for MHD fluid flow in a heterogeneous porous medium.

8. References

[1] H. Andersson, MHD flow of a viscoelastic fluid past a stretching surface, Acta Mechanica 95 (1) (1992) 227–230.

[2] P. Besthapu, R. U. Haq, S. Bandari, Q. M. Al-Mdallal, Mixed convection flow of thermally stratified MHD nanofluid over an exponentially stretching surface with viscous dissipation effect, Journal of the Taiwan Institute of Chemical Engineers 71 (2017) 307–314.

[3] W. Khan, I. Pop, Boundary-layer flow of a nanofluid past a stretching sheet, International journal of heat and mass transfer 53 (11-12) (2010) 2477–2483.

[4] T. Hayat, Z. Abbas, M. Sajid, Series solution for the upper-convected Maxwell fluid over a porous stretching plate, Physics Letters A 358 (5) (2006) 396–403.

[5] M. Ramzan, M. Bilal, J. D. Chung, Effects of thermal and solutal stratification on Jeffrey magneto-nanofluid along an inclined stretching cylinder with thermal radiation and heat generation/absorption, International Journal of Mechanical Sciences 131 (2017) 317–324.

[6] E. Elbashbeshy, M. Bazid, Heat transfer over an unsteady stretching surface, Heat and Mass Transfer 41 (1) (2004) 1–4.

[7] B. S. Dandapat, B. Santra, K. Vajravelu, The effects of variable fluid properties and thermocapillarity on the flow of a thin film on an unsteady stretching sheet, International Journal of Heat and Mass Transfer 50 (5) (2007) 991–996.

[8] A. Ahmadi, A. Zahmatkesh, M. Hatami, D. Ganji, A comprehensive analysis of the flow and heat transfer for a nanofluid over an unsteady stretching flat plate, Powder Technology 258 (2014) 125–133.

[9] M. R. Eid, K. L. Mahny, Unsteady MHD heat and mass transfer of a non-Newtonian nanofluid flow of a two-phase model over a permeable stretching wall with heat generation/absorption, Advanced Powder Technology 28 (11) (2017) 3063–3073.

[10] M. Khan, M. Azam, Unsteady heat and mass transfer mechanisms in MHD Carreau nanofluid flow, Journal of Molecular Liquids 225 (2017) 554–562.

[11] A. Hamid, M. Khan, et al., Unsteady mixed convective flow of Williamson nanofluid with heat transfer in the presence of variable thermal conductivity and magnetic field, Journal of Molecular Liquids 260 (2018) 436–446.

[12] F. Liu, I. Turner, V. Anh, An unstructured mesh finite volume method for modelling saltwater intrusion into coastal aquifers, Journal of Applied Mathematics and Computing 9 (2) (2002) 391–407.
[13] V. Volpert, Y. Nec, A. Nepomnyashchy, Fronts in anomalous diffusion–reaction systems, Philosophical Transactions of the Royal Society of London A: Mathematical, Physical and Engineering Sciences 371 (1982) (2013) 20120179.
[14] P. Szymczak, A. Ladd, Boundary conditions for stochastic solutions of the convection-diffusion equation, Physical review E 68 (3) (2003) 036704.
[15] H. Qi, X. Jiang, Solutions of the space-time fractional Cattaneo diffusion equation, Physica A: Statistical Mechanics and its Applications 390 (11) (2011) 1876–1883.
[16] S. Fedotov, V. Méndez, Non-markovian model for transport and reactions of particles in spiny dendrites, Physical review letters 101 (21) (2008) 218102.
[17] M. M. Meerschaert, A. Sikorskii, Stochastic models for fractional calculus, Vol. 43, Walter de Gruyter, 2012.
[18] L. Liu, L. Zheng, F. Liu, Time fractional Cattaneo-Christov anomalous diffusion in comb frame with finite length of fingers, Journal of Molecular Liquids 233 (2017) 326–333.
[19] X. Chen, Y. Ye, X. Zhang, L. Zheng, Lie-group similarity solution and analysis for fractional viscoelastic MHD fluid over a stretching sheet, Computers & Mathematics with Applications 75 (8) (2018) 3002–3011.
[20] M. I. Asjad, F. Miraj, I. Khan, Soret effects on simultaneous heat and mass transfer in MHD viscous fluid through a porous medium with uniform heat flux and Atangana-Baleanu fractional derivative approach, The European Physical Journal Plus 133 (6) (2018) 224.
[21] T. K. Perkins, O. C. Johnston, A Review of Diffusion and Dispersion in Porous Media, Society of Petroleum Engineers Journal 3 (3) (1963) 70–84.
[22] H. F. Lecoanet, J.-Y. Bottero, M. R. Wiesner, Laboratory assessment of the mobility of nanomaterials in porous media, Environmental Science & Technology 38 (19) (2004) 5164–5169.
[23] D. Grolimund, M. Borkovec, Colloid-facilitated transport of strongly sorbing contaminants in natural porous media: Mathematical modeling and laboratory column experiments, Environmental science & technology 39 (17) (2005) 6378–6386.
[24] U. Scheven, D. Verganelakis, R. Harris, M. Johns, L. Gladden, Quantitative nuclear magnetic resonance measurements of preasymptotic dispersion in flow through porous media, Physics of fluids 17 (11) (2005) 117107.
[25] J. Thovert, F. Wary, P. Adler, Thermal conductivity of random media and regular fractals, Journal of Applied Physics 68 (8) (1990) 3872–3883.
[26] B. Berkowitz, H. Scher, S. E. Silliman, Anomalous transport in laboratory-scale, heterogeneous porous media, Water Resources Research 36 (1) (2000) 149–158.
[27] B. Berkowitz, H. Scher, On Characterization of Anomalous Dispersion in Porous and Fractured Media, Water Resources Research 31 (6) (1995) 1461–1466.
[28] B. Berkowitz, A. Cortis, M. Dentz, H. Scher, Modeling non-Fickian transport in geological formations as a continuous time random walk, Reviews of Geophysics 44 (2) (2006) 177–186.
[29] P. De Anna, T. Le Borgne, M. Dentz, A. M. Tartakovsky, D. Bolster, P. Davy, Flow intermittency, dispersion, and correlated continuous time random walks in porous media, Physical review letters 110 (18) (2013) 184502.
[30] A. Saadatmandi, M. Dehghan, A tau approach for solution of the space fractional diffusion equation, Computers & Mathematics with Applications 62 (3) (2011) 1135–1142.
[31] K. Van Bockstal, R. H. De Staelen, M. Slodička, Identification of a memory kernel in a semilinear integrodifferential parabolic problem with applications in heat conduction with memory, Journal of Computational and Applied Mathematics 289 (2015) 196–207.
[32] M. Hamad, M. Ferdows, Similarity solution of boundary layer stagnation-point flow towards a heated porous stretching sheet saturated with a nanofluid with heat absorption/generation and suction/blowing: a Lie group analysis, Communications in Nonlinear Science and Numerical Simulation 17 (1) (2012) 132–140.

[33] S. Shen, F. Liu, Error Analysis of an Explicit Finite Difference Approximation for the Space Fractional Diffusion Equation with Insulated Ends, Anziam Journal 46 (2005) 871–887.
[34] M. Stynes, J. L. Gracia, A finite difference method for a two-point boundary value problem with a Caputo fractional derivative, IMA Journal of Numerical Analysis 35 (2) (2015) 698–721.
[35] J. L. Gracia, M. Stynes, Central difference approximation of convection in Caputo fractional derivative two-point boundary value problems, Journal of Computational and Applied Mathematics 273 (2015) 103–115.
[36] M. Pan, L. Zheng, F. Liu, X. Zhang, Modeling heat transport in nanofluids with stagnation point flow using fractional calculus, Applied Mathematical Modelling 40 (21) (2016) 8974–8984.
[37] O. Axelsson, L. Kolotilina, Monotonicity and discretization error estimates, Society for Industrial and Applied Mathematics, 1990.
[38] P. Vyas, N. Srivastava, Radiative MHD flow over a non-isothermal stretching sheet in a porous medium, Applied Mathematical Sciences 4 (50) (2010) 2475–2484.
[39] H. Scher, M. Lax, Stochastic transport in a disordered solid. I. Theory, Physical Review B 7 (10) (1973) 4491.
[40] J. Klafter, A. Blumen, M. F. Shlesinger, Stochastic pathway to anomalous diffusion, Physical Review A 35 (7) (1987) 3081.
[41] A. Compte, Stochastic foundations of fractional dynamics, Physical Review E 53 (4) (1996) 4191.
[42] M. Pan, L. Zheng, C. Liu, F. Liu, P. Lin, G. Chen, A stochastic model for thermal transport of nanofluid in porous media: Derivation and applications, Computers & Mathematics with Applications 75 (2017) 1226–1236.
[43] R. Metzler, J. Klafter, The random walk's guide to anomalous diffusion: a fractional dynamics approach, Physics reports 339 (1) (2000) 1–77.
[44] R. Metzler, J. Klafter, I. M. Sokolov, Anomalous transport in external fields: Continuous time random walks and fractional diffusion equations extended, Physical Review E 58 (2) (1998) 1621.
[45] N. Krepysheva, L. Di Pietro, M.-C. Néel, Space-fractional advection-diffusion and reflective boundary condition, Physical Review E 73 (2) (2006) 021104.
[46] D. A. Benson, S. W. Wheatcraft, M. M. Meerschaert, Application of a fractional advection-dispersion equation, Water Resources Research 36 (6) (2000) 1403–1412.
[47] M. G. Herrick, D. A. Benson, M. M. Meerschaert, K. R. Mccall, Hydraulic conductivity, velocity, and the order of the fractional dispersion derivative in a highly heterogeneous system, Water Resources Research 38 (11) (2002) 1227–1239.
[48] F. Zeng, F. Liu, C. Li, K. Burrage, I. Turner, V. Anh, A Crank–Nicolson ADI spectral method for a two-dimensional Riesz space fractional nonlinear reaction-diffusion equation, SIAM Journal on Numerical Analysis 52 (6) (2014) 2599–2622.
[49] M. Pan, L. Zheng, F. Liu, C. Liu, X. Chen, A spatial-fractional thermal transport model for nanofluid in porous media, Applied Mathematical Modelling 53 (2018) 622–634.

Figures

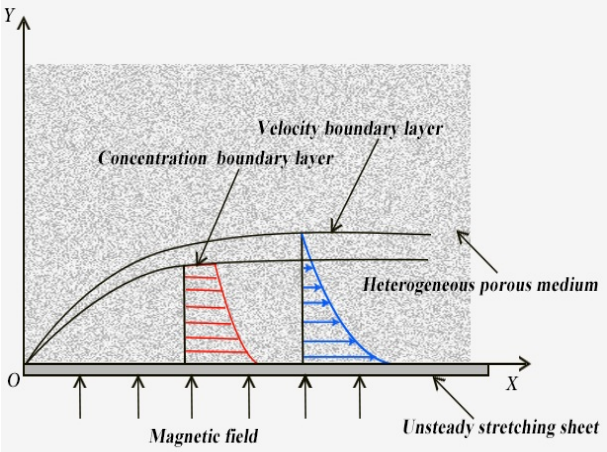

Fig. 1: The physical model of unsteady stretching sheet in a heterogeneous porous medium.

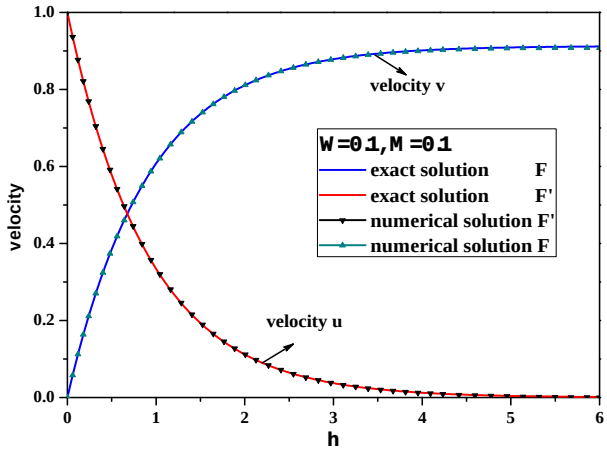

Fig. 2: The numerical solutions and exact solutions comparison for the velocity profiles with the conditions t=6 (steady).

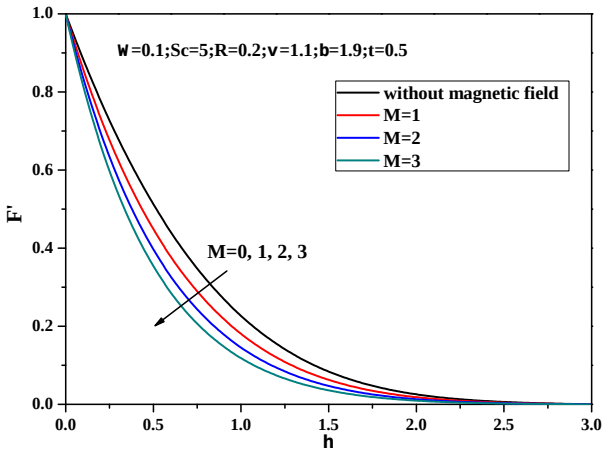

Fig. 3: Effects of Hartmann number on velocity with the conditions $\Omega = 0.1; Sc = 5; R = 0.2; \varpi = 1.1; \beta = 1.9; t = 0.5$.

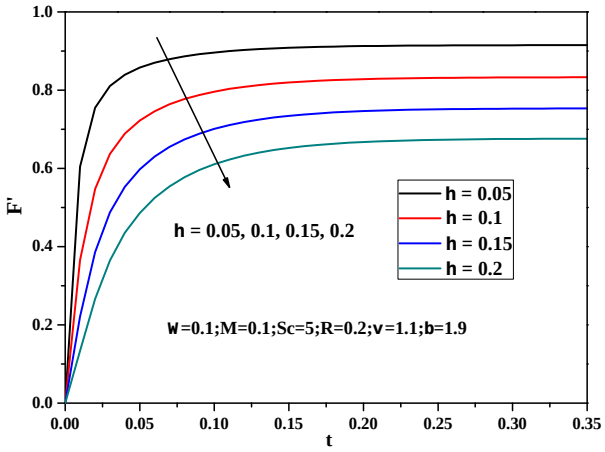

Fig. 4: Effects of time parameter and similarity variable η on velocity with the conditions $M = 0.1; \Omega = 0.1; Sc = 5; R = 0.2; \varpi = 1.1; \beta = 1.9$.

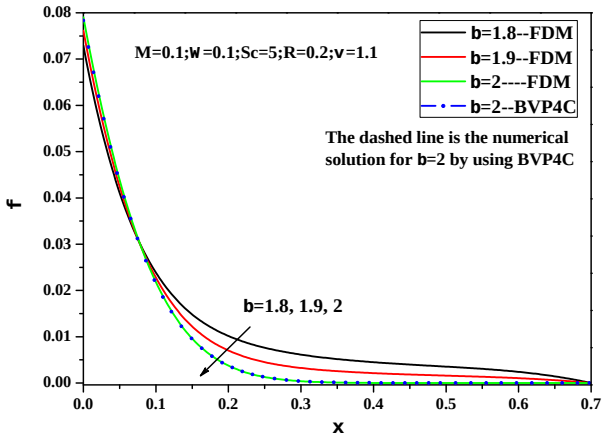

Fig. 5: Effects of fractional derivative parameter on concentration with the conditions $M = 0.1; \Omega = 0.1; Sc = 5; R = 0.2; \varpi = 1.1; t = 1$.

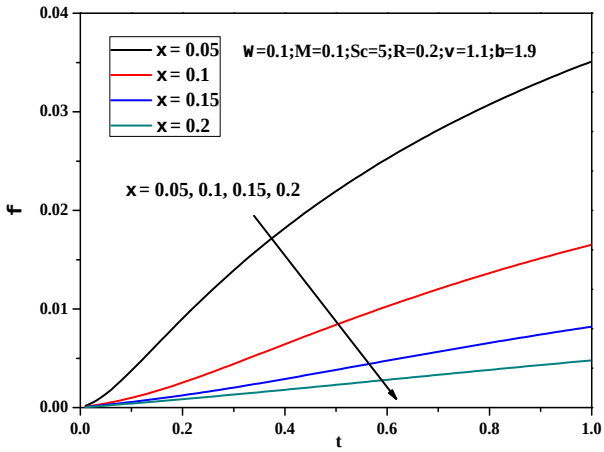

Fig. 6: Effects of time parameter and similarity variable ξ on concentration with the conditions $M = 0.1; \Omega = 0.1; Sc = 5; R = 0.2; \varpi = 1.1; \beta = 1.9$.

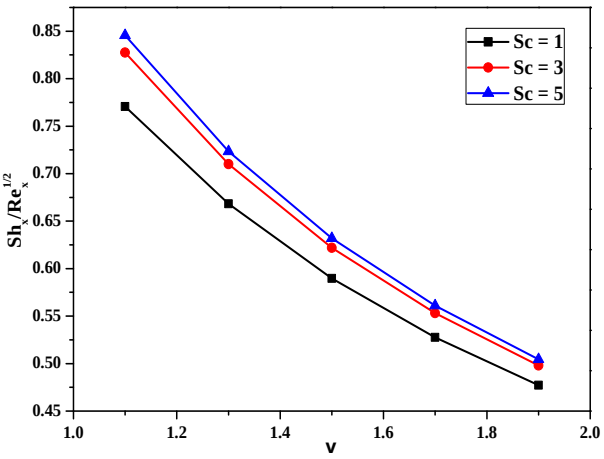

Fig. 7: Effects of Schmidt number and scaled convective mass transfer parameter on local Sherwood number with the conditions $M = 0.1; \Omega = 0.1; R = 0.2; \beta = 1.9; t = 1$.

Table 1: Skin friction coefficient distributions for different M and Ω with $t = 1$.

$C_f Re_x^{1/2}$		Ω				
		0	1	2	3	4
M	0.2	-1.3991	-1.6636	-1.9053	-2.1283	-2.3356
	0.4	-1.4540	-1.7136	-1.9513	-2.1709	-2.3754
	0.6	-1.5079	-1.7627	-1.9966	-2.2130	-2.4147
	0.8	-1.5608	-1.8111	-2.0412	-2.2544	-2.4535

Table 2: Sherwood number distributions for different R and β with $t = 1$.

$Sh_x/Re_x^{1/2}$		β				
		1.8	1.85	1.9	1.95	2
R	0.2	0.8476	0.8464	0.8453	0.8443	0.8434
	0.4	0.8510	0.8498	0.8487	0.8477	0.8467
	0.6	0.8541	0.8529	0.8517	0.8507	0.8496
	0.8	0.8568	0.8556	0.8544	0.8534	0.8523